Available online at www.sciencedirect.com
ScienceDirect
Mendeleev Commun., 2017, **27**, 101–103
Mendeleev Communications

Relative contribution of gas dynamic and chemical factors to flame penetration through small openings in a closed cylindrical reactor

Nikolai M. Rubtsov,*[a] Victor I. Chernysh,[a] Georgii I. Tsvetkov[a] and Kirill Ya. Troshin[b]

[a] *Institute of Structural Macrokinetics and Materials Science, Russian Academy of Sciences, 142432 Chernogolovka, Moscow Region, Russian Federation. Fax: +7 495 962 8025; e-mail: nmrubtss@mail.ru*
[b] *N. N. Semenov Institute of Chemical Physics, Russian Academy of Sciences, 119991 Moscow, Russian Federation*

DOI: 10.1016/j.mencom.2017.01.034

The ignition of a dilute stoichiometric methane–oxygen mixture (total pressure, up to 200 Torr) occurs behind a single opening on the transition of a laminar flow to a turbulent one rather than after a delay period of ignition.

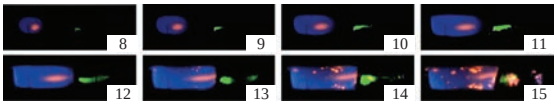

The theoretical description of the inception and growth of instabilities in laminar shear flows that lead to a transition to turbulence is an unsolved problem of fluid mechanics. This is an extraordinarily complicated process, which is not fully understood. Despite long-term systematic experimental and theoretical studies, the cause of an infringement of a laminar gas flow, *e.g.*, in the presence of obstacles in round pipes and the emergence of turbulence, remains unclear.[1,2]

In case of ignition after a possible failure of any gas infrastructure at industrial or civil sites, the pressure load due to fast propagating flames can endanger the integrity of a building.[3–6] Although the global characteristics of flame acceleration have been investigated,[7–11] the data obtained by locally highly resolved measurement methods determining process variables like density, temperature, velocity, and species concentration are still very poor. This is due to the fact that the required resolution in time and space cannot be achieved even by the use of modern optical methods for highly transient processes.[3]

Previously,[8,9] the combustion of lean hydrogen–air mixtures was studied in the presence of highly blocking obstacles substituting an opening between two rooms. The extinction of a hydrogen flame in the jet area has to be expected even at concentrations much higher than the flammability limit of the mixture. In addition, it was experimentally shown[12] that an acoustic resonator like Helmholtz's resonator connected with a cylindrical reactor can provide a significant flame acceleration under spark initiation in lean (15%) hydrogen–oxygen mixtures close to the lower detonation limit. This is very important for both solution to problems of explosion safety and the validation of computer codes simulating these accidents.

Recently, we found[13] that the ignition of methane–oxygen mixture (total pressure, up to 200 Torr) after a single obstacle with a small circular opening is observed markedly far from an obstacle surface. The meshed sphere as an opening leads to increase in the length of a flame jump through the obstacle as compared to the round opening. We mean by flame jump the distance of flame front emergence behind an obstacle. The symmetry of the openings allowed 2D modeling to be used; however, flame penetration modeling through a rectangular opening calls for a 3D approach. Thus, it is important to obtain reliable experimental data on the penetration of a flame front (FF) through a small rectangular opening.

It was shown[14,15] that the active centers of methane and hydrogen combustion, which determine flame propagation, are chemically different. Thus, the termination of active intermediates on the obstacle surface contributes significantly to the interaction of FF with obstacles in natural gas–air mixtures, *i.e.*, the role of active intermediates is very important in the process.[9,10]

Here, we report experimental results on flame propagation through circular and rectangular openings in a cylindrical channel. The aim of this work was to study FF penetration through rectangular openings in comparison with circular ones with the use of both color speed cinematography and the visualization of gas currents by the illumination of inert fine powder with a laser sheet. Thus, the concerned combustion phenomenon is the acceleration of an initially slow flame by single obstacles with small circular and rectangular openings of different blockage ratios for dilute stoichiometric methane–air mixtures to understand the influence of the local geometry.

Flame propagation in the stoichiometric mixtures of methane with oxygen diluted with CO_2 or Kr at initial pressures of 100–200 Torr and 298 K in a horizontal cylindrical quartz reactor 70 cm in length and 14 cm in diameter was investigated. The reactor was fixed in two stainless steel gateways at butt-ends supplied with inlets for gas pumping and blousing and a safety shutter, which swung outward when the total pressure in the reactor exceeded 1 atm.[13] A pair of spark ignition electrodes was located near the left butt-end of the reactor (see Figure S1, Online Supplementary Materials). Thin obstacles with rectangular openings (7 and 10 mm width and 65 mm in length) or circular openings 20 and 25 mm in diameter were placed vertically at the center of the reactor. In certain experiments, the circular opening 20 mm in diameter and the rectangular opening 10 mm wide and 65 mm long were closed by iron mesh with 0.5 mm cells (wire diameter, 0.25 mm). The illumination of fine $MgCO_3$ particles, which are blown out from the reservoir through an opening with gas current at flame propagation from left to right, was carried out by means of a laser sheet. The combustible mixture (15.4% CH_4 + 30.8% O_2 + 46% CO_2 + 7.8% Kr) was prepared; CO_2 was added to enhance the quality of filming by decreasing

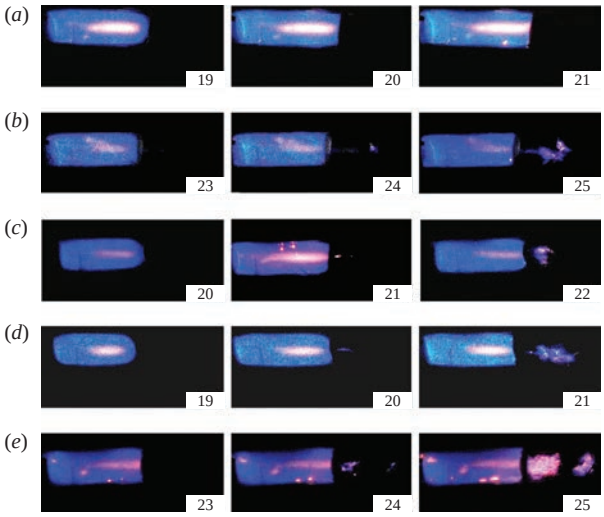

Figure 1 High-speed filming of FF propagation through (*a*) the rectangular opening (slit) 7 mm wide and 65 mm long, (*b*) an opening 25 mm in diameter, a rectangular opening 10 mm wide and 65 mm long: (*c*) the slit was placed vertically, (*d*) the slit was placed horizontally and (*e*) the slit was placed vertically and closed by iron mesh. Initial pressure, 170 Torr. The figure on a frame corresponds to a frame number after discharge.

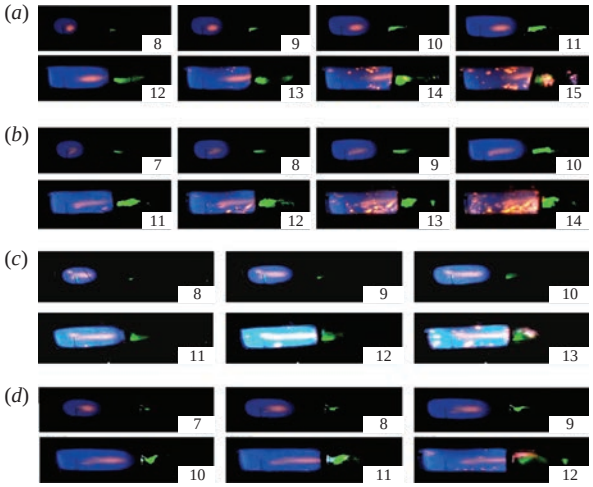

Figure 2 Speed filming of FF and visualization of gas current through (*a*) a circular opening (d = 20 mm), (*b*) a circular meshed opening (d = 20 mm), a rectangular opening 10 mm wide and 65 mm long: (*c*) vertically placed slit and (*d*) vertically placed slit closed by iron mesh. Initial pressure, 170 Torr. The figure on a frame corresponds to frame number after discharge, 300 frames per second.

FF velocity; Kr was added to diminish the discharge threshold. The reactor was filled with the mixture to a necessary pressure. Then, spark initiation was performed (discharge energy, 1.5 J). Speed filming of ignition dynamics and FF propagation was carried out from the side of the reactor with a Casio Exilim F1 Pro digital camera (frame frequency, 600 s^{-1}).[14–16] The video file was stored in computer memory and its time-lapse processing was performed.[15] Chemically pure reagents were used.

Flame propagation through circular and rectangular openings in methane–oxygen mixtures is shown in Figure 1. The FF does not penetrate through the obstacle; therefore, the limit on penetration exists because FF successfully propagates through a 10 mm wide opening [Figure 1(*c*)]. The first spot of ignition is observed near the obstacle surface as distinct from FF propagation through a round opening [Figure 1(*b*)] behind which a flame jump is observed. Figure 1(*d*) (frames 24, 25) shows the second flame jump in the presence of the mesh placed on 10 mm wide rectangular opening.

The accumulation of free radicals behind the obstacle was detected experimentally. The mixing of these radicals with unburned gas enhances the explosiveness of the mixture[9,10] due to chain branched combustion processes.[8,12,13]

Figure 2 shows the gas currents detected by the illumination of $MgCO_3$ fine particles by a laser sheet, which was blown out with expanding gas from the reservoir (see Figure S1) through both circular and rectangular openings. The density in the flow after the obstacle exhibits two maxima near the obstacle and far from the obstacle surface. The position of the second maximum correlates with the length of the flame jump through the corresponding obstacle.

Shot sequences of a gas current through the rectangular opening and high-speed filming of a gas current through the rectangular opening closed by iron mesh are also shown in Figure 2. In a similar way to FF penetration through circular openings, the density in the flow after obstacle reveals two maxima. The second flame jump is observed at a greater distance in the presence of the mesh.

To determine major factors influencing the flame jump at FF penetration through a small opening, it is reasonable to compare the penetration of FF through circular and rectangular openings. Apparently, as can be seen in Figure 2, long before the contact of FF with the obstacle, fine particles illuminated by the laser sheet already start moving [Figure 2(*a*), shot 8; Figure 2(*b*), shot 7; Figure 2(*c*), shot 8; Figure 2(*d*), shot 7]. Therefore, an initially undisturbed submerged axisymmetric or plain jet is formed in the gas behind an obstacle [Figure 2(*b*), shots 7–9 and Figure 2(*c*), shots 8–10, respectively].

After a contact of FF with the obstacle, the primary ignition centers (the local volumes containing both the active centers of combustion[9,10] and the gas heated to combustion temperature) arise in this submerged jet. It is believed that these primary centers move in the submerged jet during the delay period (induction period) of ignition; then, the ignition occurs. It is inconsistent with data published by Jourdan *et al.*[10] who claimed that, at passing the orifice by FF, the high turbulence intensities in the turbulent jet lead to quenching effects resulting in an extinction of the flame immediately behind the orifice.

Let us roughly estimate the time t of primary center movement in the submerged jet in an incompressible flow approximation.[17] For the axial velocity component v_L in a plane-parallel stream $v_L/v_0 = 1.2/(0.1x/L - 0.41)^{1/2}$; and in an axisymmetric stream $v_R/v_0 = 0.96/(0.07x/R - 0.29)$. Here, v_0 is the flame velocity at the moment of contact of FF with the obstacle, x is the coordinate, L is the rectangular slit width, R is the radius of the circular opening, and numerical values are published empirical parameters.[17] Then,

$$t_L = \int_{0.41}^{X} \frac{\mathrm{d}x}{v_L/v_0}$$

and

$$t_R = \int_{0.96}^{X} \frac{\mathrm{d}x}{v_R/v_0}.$$

The t_R/t_L relation[17] for equal values of upper integration limit X = 10, makes ~4; for X = 3, makes ~2. It means that, in a plane-parallel stream, the primary center travels a distance of X for the time much shorter than that in an axisymmetric stream; therefore, during the delay period of ignition, the primary center will move away farther from the obstacle, as compared to the case of the axisymmetric stream. On the other hand, the experiment has shown [*cf.* Figure 2(*b*),(*d*)] that the ignition behind the opening occurs earlier when FF passes the rectangular opening, than in the case of the circular opening. It means that if the flame jump

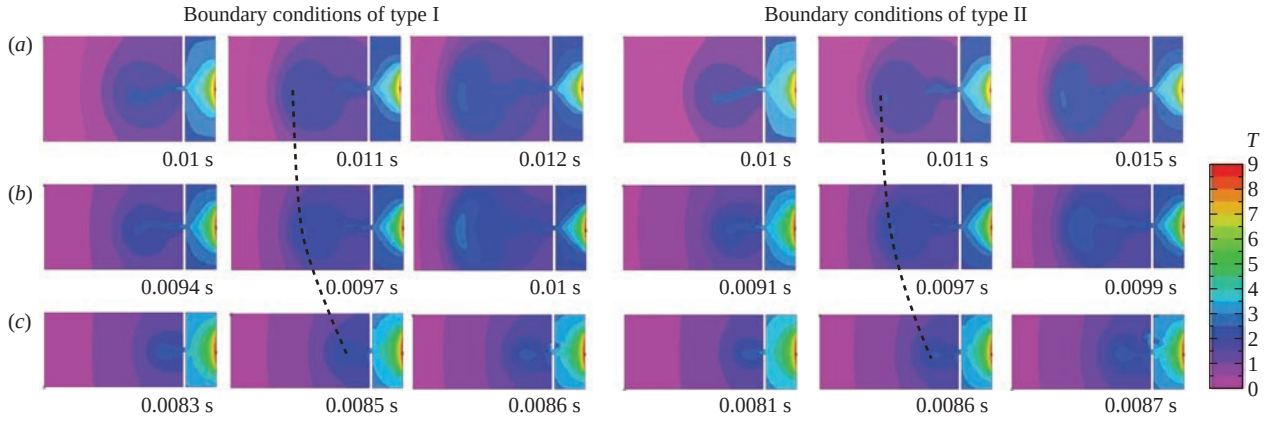

Figure 3 Results of the calculation of flame propagation through a single orifice, channel widths of (*a*) 1, (*b*) 0.8 and (*c*) 0.6 dimensionless units. Change in dimensionless temperature for flame propagation through a single opening for $n_\xi = 0$ (boundary conditions of type I) and $n = 0$ (boundary conditions of type II). The scale of dimensionless temperature is presented on the right.

length was determined by the delay period of ignition, it would be smaller for the circular opening contrary to the experiment.

In our opinion, another explanation can be proposed. Recently, Lemanov *et al.*[18] determined the coordinates of laminar and turbulent transition in a submerged jet for both flat and round streams at different Reynolds numbers by means of visualization and measurements by a heat-loss anemometer. They found that the length of the laminar part in flat streams is considerably (by a factor of 2–5) less than in the round one. It gives the grounds to assume that the flame jump length in the submerged jet formed after the opening is determined by the time of occurrence of the transition from the laminar flow to the turbulent one rather than the time of ignition delay period in the flammable mixture. The relatively weak influence of the overall reaction rate on the flame jump length is another reason for the above explanation. We approximately illustrated the contribution of gas dynamic and chemical factors by numerical modeling using compressible dimensionless reactive Navier–Stokes equations in a low Mach number approximation,[16–21] which describe flame propagation in a two-dimensional channel. Flame propagation in three channels of different widths was analyzed. The problem was solved by finite element analysis with the FlexPDE 6.08 package.[22] The initiation condition was taken as $T = 10$ on the right boundary of the channel with a vertical orifice. The boundary conditions were $C_\xi = 0$, $u = 0$, $v = 0$, $\rho_\xi = 0$, $n_\xi = 0$ (Figure 3, boundary conditions of type I), $n = 0$ (Figure 3, boundary conditions of type II), and convective heat exchange $T_t = T - T_0$, where ξ is a dimensionless coordinate (x,y). The results of calculations of flame propagation through the orifice are shown in Figure 3. The available data reveal an increase in the time of occurrence of a laminar-to-turbulent flow transition in pipes with increasing pipe diameter in agreement with published data.[24] Therefore, as Figure 3 indicates, the results of numerical calculations testify in favor of a primary contribution of gas dynamic factors to the flame jump length.

The results are important for both 3D modeling and the solution of explosion safety problems for volumes with complex geometry.

Online Supplementary Materials

Supplementary data associated with this article can be found in the online version at doi:10.1016/j.mencom.2017.01.034.

References

1 S. A. Orzag and L. C. Kellst, *J. Fluid Mech.*, 1980, **96**, 159.
2 W. S. Saric, H. L. Reed and E. J. Kerschen, *Annu. Rev. Fluid Mech.*, 2002, **34**, 291.
3 B. Durst, N. Ardey and F. Mayinger, in *Proceedings of the International Cooperative Exchange Meeting on Hydrogen and Reactor Safety*, Toronto, 1997, p. 34.
4 G. K. Hargrave, S. J. Jarvis and T. C. Williams, *Meas. Sci. Technol.*, 2002, **13**, 1036.
5 R. G. Abdel-Gayed, D. Bradley and F. K.-K. Lung, *Combust. Flame*, 1989, **76**, 213.
6 S. S. Ibrahim and A. R. Masri, *J. Loss Prev. Proc. Ind.*, 2001, **14**, 213.
7 G. D. Salamandra, T. V. Bazhenova and I. M. Naboko, *Zh. Tekh. Fiz.*, 1959, **29**, 1354 (in Russian).
8 C. Clanet and G. Searby, *Combust. Flame*, 1996, **105**, 225.
9 N. Ardey and F. Mayinger, in *Proceedings of the 1st Trabson International Energy and Environment Symposium*, Karadeniz Technical University, Trabson, Turkey, 1996, p. 679.
10 M. Jourdan, N. Ardey, F. Mayinger and M. Carcassi, in *Proceedings of 11th IHTC*, Kuongju, Korea, 1998, vol. 7, p. 295.
11 R. Kh. Abdullin, V. S. Babkin and P. K. Senachin, *Fiz. Goreniya Vzryva*, 1988, **24**, 3 (in Russian).
12 N. M. Rubtsov, A. N. Vinogradov, A. P. Kalinin, A. I. Rodionov, K. Ya. Troshin and G. I. Tsvetkov, *Mendeleev Commun.*, 2015, **25**, 482.
13 N. M. Rubtsov, B. S. Seplyarskii, I. M. Naboko, V. I. Chernysh, G. I. Tsvetkov and K. Ya. Troshin, *Mendeleev Commun.*, 2015, **25**, 304.
14 N. M. Rubtsov, V. I. Chernysh, G. I. Tsvetkov and B. S. Seplyarskii, *Int. J. Chem. Mater. Res.*, 2014, **2**, 102.
15 N. M. Rubtsov, B. S. Sepljarsky, I. M. Naboko, V. I. Chernysh and G. I. Tsvetkov, *J. Aeronaut. Aerospace Eng.*, 2013, **2**, 127.
16 I. M. Naboko, N. M. Rubtsov, B. S. Seplyarskii, K. Ya. Troshin, V. I. Chernysh and G. I. Tsvetkov, *Mendeleev Commun.*, 2013, **23**, 358.
17 G. N. Abramovich, *Teoriya turbulentnykh strui (The Theory of Turbulent Flows)*, 1960, reprint, Ekolit, Moscow, 2011 (in Russian).
18 V. V. Lemanov, V. I. Terekhov, K. A. Sharov and A. A. Shumeiko, *Tech. Phys. Lett.*, 2013, **39**, 421 (*Pis'ma ZhTF*, 2013, **39**, 34).
19 A. Majda, *Equations for Low Mach Number Combustion*, Center for Pure and Applied Mathematics, University of California, Berkeley, 1982, PAM-112.
20 N. M. Rubtsov, B. S. Seplyarskii, I. M. Naboko, V. I. Chernysh, G. I. Tsvetkov and K. Ya. Troshin, *Mendeleev Commun.*, 2014, **24**, 308.
21 V. Akkerman, V. Bychkov, A. Petchenko and L.-E. Eriksson, *Combust. Flame*, 2006, **145**, 206.
22 G. Backstrom, *Simple Fields of Physics by Finite Element Analysis*, GB Publishing, 2005.
23 B. Lewis and G. von Elbe, *Combustion, Flames and Explosions of Gases*, Academic Press, New York, 1987.
24 F. Durst, K. Haddad and Ö. Ertunç, in *Advances in Turbulence XII*, ed. B. Eckhardt, Springer, 2009, p. 131.

Received: 6th June 2016; Com. 16/4950